Green Chemistry

Accepted Manuscript

ROYAL SOCIETY OF CHEMISTRY

www.rsc.org/greenchem

Cite this: DOI: 10.1039/c0xx00000x

www.rsc.org/xxxxxx

ARTICLE TYPE

Polymer@silica composites with tunable outer and inner surface properties: a platform for aqueous asymmetric transfer hydrogenation

Xiaoming Zhang, [a, b] Yaopeng Zhao, [a] Juan Peng, [a, b] and Qihua Yang*[a]

Received (in XXX, XXX) Xth XXXXXXXXX 20XX, Accepted Xth XXXXXXXXX 20XX

DOI: 10.1039/b000000x

A highly efficient chiral solid catalyst was synthesized via *in situ* polymerization of chiral monomer (1R, 2R)-N[1]-(4-vinylbenzenesulfonyl)-1, 2-diphenylethane-1, 2-diamine (VBS-DPEN) together with divinylbenzene (DVB) in the nanocages of mesoporous silica (FDU-12) followed by coordination with metal precursor $[Cp^*RhCl_2]_2$ (Cp^*=pentamethylcyclopentadiene). The solid chiral catalyst with hydrophilic outer and hydrophobic inner surface properties could be well dispersed in aqueous solution and facilitate the adsorption of hydrophobic ketones in aqueous solution. As a result, it could efficiently catalyze the aqueous asymmetric transfer hydrogenation (ATH) of ketones to afford 94% ee and much higher TOF than homogeneous Rh-TsDPEN (TOF 585 versus 340 h^{-1}). Our studies suggest that the dispersion of polymers in the nanopores of mesoporous silica could provide a new approach for the synthesis of high performance solid catalyst for organic reactions in water.

Introduction

The aqueous asymmetric transfer hydrogenation (ATH) reaction catalyzed by Noyori-Ikariya catalyst (Rh, Ru, or Ir complexes of TsDPEN) has attracted considerable attentions due to the advantages of the high catalytic performance of the reaction system, operational simplicity, safety, and the easy availability of reductants.[1-6] However, practical applications are still hindered because of the difficulty in separation and reuse of the expensive catalyst, which will lead to a high cost and even a heavy pollution from metallic ions. Although several strategies have been developed for the immobilization of the homogeneous catalyst on polymer or inorganic materials, the obtained heterogeneous catalyst often exhibits lower activity than the corresponding homogeneous catalyst owing to uncontrollable hindrance and changes in the chiral microenvironment of active sites.[7-10] Moreover, the ATH reaction in water involves water-oil-solid tri-phase situations, and the surface properties of the solid catalyst should be carefully tuned. Different types of surfactant have been employed for accelerating the diffusion rate of substrates and products through solid catalysts.[11, 12] However, the addition of surfactants will increase the cost and difficulties in product purification. Thus, the surface modification of solid catalyst for accelerating the diffusion rates of different types of substrates has attracted much research attention.[13, 14]

Recently, different strategies have been employed for the synthesis of high performance solid chiral catalysts for aqueous ATH reaction without the addition of surfactants.[15-18] For example, Li and co-workers reported that Rh-TsDPEN immobilized in mesoporous silicas with surfactant partially removed could efficiently catalyze the aqueous ATH reaction, in which the surfactants in the nanopore of mesoporous silicas could act as a phase transfer agent.[19-21] Xiao and co-workers recently demonstrated that Ru-TsDPEN supported on mesoporous polymers shows high activity in aqueous ATH reaction because the mesoporous polymer with superhydrophobicity could efficiently enrich the lipophilic substrates.[22] Our group previously reported that amphiphilic surface modification of mesoporous silicas accommodated with Ru-TsDPEN could efficiently improve the catalytic activity of solid chiral catalysts for aqueous ATH reaction.[14] Though the strategies mentioned above have been proved to be efficient, developing new and cost efficient strategies is still highly desirable for further improving the efficiency and stability of the solid catalysts.

Polymer@silica composite materials with combined advantages of both organic polymer (e.g., flexibility, ductility, and processibility) and inorganic material (e.g., rigidity, thermal stability) have been widely used in the fields of drug delivery, absorption of organic pollutants, catalysis, sensing and so on.[23-29] In particular, the physical and chemical properties, especially the surface hydrophobicity/hydrophilicity of the composite materials can be easily tailored by changing the composition of polymers, the content of polymer coating, and the degree of polymer cross-linking. With these valuable advantages, the polymer@silica nanocomposite material with tunable surface properties might have great potential in catalysis, especially using water as solvent. However, the application of polymer@silica nanocomposite material in aqueous asymmetric catalysis has seldom been reported as far as we know.

Herein, we report the construction of a highly efficient chiral solid catalyst with tunable outer and inner surface properties for aqueous asymmetric transfer hydrogenation reactions by polymerization of divinylbenzene (DVB) and chiral monomer (1R, 2R)-N[1]-(4-vinylbenzenesulfonyl)-1, 2-diphenylethane-1, 2-

diamine (VBS-DPEN) in the nanopores of mesoporous silica (FDU-12). After coordination with $[Cp^*RhCl_2]_2$ (Cp^*=pentamethylcyclopentadiene), the chiral solid catalyst could efficiently catalyze the aqueous ATH reactions in the absence of phase transfer agents and co-solvents, and exhibits much higher activity than homogeneous counterpart (TOF 585 versus 340 h^{-1}), probably due to the co-existence of hydrophobic polymer and hydrophilic silica which could provide a suitable accommodation microenvironment for both hydrophilic and hydrophobic reactant molecules.

Experimental Section

Chemicals and materials

All chemicals were used as received unless otherwise stated. Pluronic F127 ($EO_{106}PO_{70}EO_{106}$) was purchased from Sigma Aldrich. Tetraethylorthosilicate (TEOS, AR), 1, 3, 5-trimethylbenzene (TMB), thionyl chloride ($SOCl_2$), and 4-vinylbenzenesulfinic acid sodium salt were purchased from Shanghai Chemical Reagent Company of the Chinese Medicine Group. Divinylbenzene (DVB) 80% was purchased from Aladdin-reagent Company. (1R, 2R)-1, 2-Diphenylethyldiamine [(R, R)-DPEN] was purchased from Beijing Ouhe Science and Technology Company. $[Cp^*RhCl_2]_2$ (Cp^*=pentamethylcyclo pentadiene) was purchased from Alfa Aesar. The chiral ligand (1R, 2R)-N^1-(4-vinyl-benzenesulfonyl)-1, 2-diphenylethane-1, 2-diamine (VBS-DPEN) and (1R, 2R)-N-(p-toluenesulfonyl)-1, 2-diphenylethylenediamine (TsDPEN) were synthesized according to the literature method.[13] FDU-12 was synthesized according to the reported method.[30]

Preparation of polymer@silica nanoreactor

Divinylbenzene (DVB) was purified on an alumina column to remove the polymerization inhibitors. Typically, desired amount of DVB and VBS-DPEN mixtures (0.09 or 0.17 or 0.35 or 0.70 g; molar ratio of DVB/VBS-DPEN of 4: 1) and 2, 2′-azobisisobutyronitrile (AIBN, 3% relative to total vinyl group) were dissolved in 1.5 ml of N, N-dimethylformamide (DMF). Then, the above solution was added to 1.0 g of mesoporous silicas activated by vacuum degassing at 120 ^oC for 3 h through impregnation method. The mixture was subjected to freeze-vacuum-thaw to remove the air. Then, the mixture was heated at 80 ^oC for 20 h for the polymerization of DVB and VBS-DPEN. After thoroughly washing with dichloromethane and ethanol to remove the unreacted monomers and oligomers, the sample was dried under vacuum. The samples were denoted as polymer@silica-x, where x is the weight ratio of monomers/FDU-12. For example, polymer@silica-0.35 refers to the sample synthesized using 0.35 g of monomer (DVB and VBS-DPEN with molar ratio of DVB/VBS-DPEN of 4: 1) and 1.0 g of FDU-12 during the synthesis. $Polymer_H$@silica-0.17 was synthesized in a similar condition to polymer@silica-0.17 except that the molar ratio of DVB/VBS-DPEN is different (the ratio is about 11). The mass of chiral ligand VBS-DPEN was halved, and the cut mass was replaced by DVB.

Surface modification of polymer@silica with propyl group or trimethylammonium chloride group

For further surface modification, polymer@silica-0.17 (0.5 g) was dispersed in 5 ml of hexane and 1 ml of Et_3N, followed by the addition of 3-(trimethoxysily)propyl-trimethylammonium chloride (0.5 mmol, 50 wt% methanol solution) or n-propyltrimethoxysilane (1 mmol). The mixture was refluxed for 12 h under Ar atmosphere. The solid product was isolated through centrifugation, washed with hexane and EtOH, dried under vacuum. The sample modified with 3-(trimethoxysily)propyl-trimethylammonium chloride and n-propyltrimethoxysilane as silane precursor was denoted as N^+Cl^--polymer@silica-0.17 and C_3-polymer@silica-0.17, respectively.

Preparation of solid catalysts by coordination of polymer@silica with $[Cp^*RhCl_2]_2$

In a typical procedure, polymer@silica containing 50 μmol of TsDPEN was dispersed in a mixture of dry dichloromethane (4.0 ml) and of Et_3N (0.4 ml) followed by the addition of $[Cp^*RhCl_2]_2$ (50 μmol) at room temperature. The resulting mixture was stirred at room temperature for 12 h. After filtration, the solid product was washed with excessive CH_2Cl_2 and dried under vacuum. The sample was denoted as Rh-polymer@silica-x.

Characterization

XRD patterns were recorded on a Rigaku RINT D/Max-2500 powder diffraction system by using $Cu_{K\alpha}$ radiation. Nitrogen physical adsorption measurement was carried out on micrometritics ASAP2020 volumetric adsorption analyzer. Before the measurements, the samples were out gassed at 393 K for 5 h. The BET surface area was evaluated from the data in the relative pressure range P/P_0 of 0.05 to 0.25. The total pore volume was estimated from the amount adsorbed at the P/P0 value of 0.99. The pore diameter was determined from the adsorption branch by the BJH method. Thermogravimetric analysis (TGA) was performed under an air atmosphere with a heating rate of 5 ^oC/min by using a NETZSCH STA-449F3 thermogravimetric analyzer. Transmission electron microscopy (TEM) was performed using an FEI Tecnai G2 Spirit at an acceleration voltage of 120 kV. Elemental analysis was performed with a Carlo Erba 1106 Elemental Analyzer. X-ray photoelectron spectroscopy (XPS) measurements were performed on a VG ESCALAB MK2 system, using aluminium Kα X-ray source at 250 W and 12.5 kV. The bonding energies were calibrated by using the contaminant carbon (C_{1s}=284.6 ev) as a reference.

General procedure for the asymmetric transfer hydrogenation reaction

The solid catalyst (2.5 μmol of Rh), HCOONa (0.17 g, 2.5 mmol), ketone (0.5 mmol) and water (2.0 ml) were added in a Schlenk tube (10 ml) under Ar atmosphere. After the mixture was stirred at 313K for a given period, the solid catalyst was separated via centrifugation. The aqueous solution was extracted by Et_2O for analysis of conversion and ee. The conversion and ee values were determined by chiral GC using a Supelco β-Dex 120 chiral column.

For the recycle experiment, acetophenone was chosen as substrate. The solid catalyst was separated by centrifugation and another portion of acetophenone (0.5 mmol), HCOONa (0.17 g, 2.5 mmol) and degassed water (2.0 ml) were added. The reactions were conducted at 40 ^oC for 3-14 h.

Results and Discussion

Synthesis of polymer@silica nanoreactors

High quality host material FDU-12 was selected in this study because of its three-dimensional periodic mesoporous structure and large pore size. Polymer@silica was straightforwardly constructed through *in situ* radical polymerization of DVB and VBS-DPEN monomers loaded inside nanocages of FDU-12 as shown in Scheme 1. DVB is used as both monomer and cross linker to increase the cross linking degree which will be beneficial for the stability of polymer within the nanocages. The monomers (DVB and VBS-DPEN) and initiator were introduced into the nanocages of FDU-12 via a wet impregnation method, followed by equilibration under reduced pressure in order to achieve uniform distribution. Subsequently, the monomers adsorbed in the nanocages of FDU-12 were polymerized with heating in the nanocages of FDU-12. Finally, the composite materials were washed with dichloromethane and ethanol to remove the unreacted monomers and polymers loosely adsorbed on the outer surface of FDU-12.

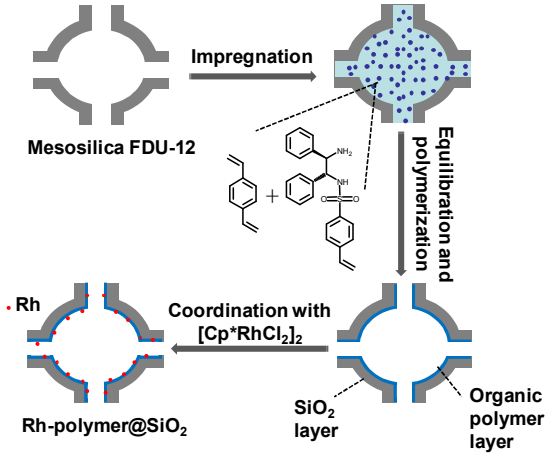

Scheme 1. Schematic illustration for the preparation of solid composite catalyst Rh-polymer@silica.

Structural characterizations

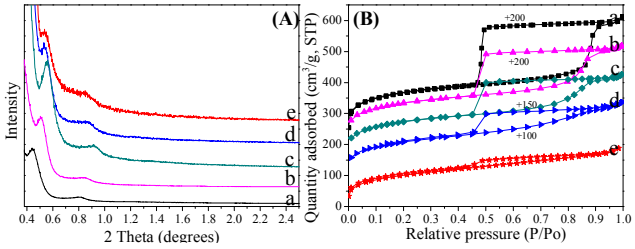

Figure 1. (A) Low angle powder X-ray diffraction patterns and (B) N_2 sorption isotherms of (a) FDU-12, (b) polymer@silica-0.09, (c) polymer @silica-0.17, (d) polymer@silica-0.35, and (e) polymer@silica-0.70.

The mesostructure of polymer@silica materials was characterized by low angle powder XRD. As shown in Figure 1, the parent FDU-12 shows an intense peak corresponding to (111) reflection along with a shoulder peak assigned to (311) reflection, showing FDU-12 has cubic Fm3m symmetry. Polymer@silica has similar XRD pattern to parent FDU-12, suggesting that all composite materials have ordered mesoporous structure with Fm3m symmetry. As the polymer loading increases, the diffraction peaks shift to higher diffraction angles, indicating that the lattice shrinkage occurs during the polymerization process.[23]

The textural properties of FDU-12 and polymer@silica composite materials are detected by the N_2 sorption experiment, and the results are summarized in Table 1. All the polymer@silica samples exhibit type IV N_2 sorption isotherm with H2 type hysteresis loop similar to FDU-12 (Figure 1B), showing that the cage-like mesostructure was well retained after inclusion of the polymer, which is consistent with the XRD results. As the polymer content increases, the H2 hysteresis loop becomes less defined and the sharp decrease in the BET surface area, pore diameter and pore volume could be observed, probably due to the occupation of polymer in the nanocages (Table 1). Notably, increasing the polymer content, the pore size decreased from 17.6 nm to 14.6 nm, 12.2 nm, 9.5 nm, respectively. If considering that all the polymers are closely adhered in the inner surface of nanocages of FDU-12, the thickness of polymer should be 1.5 nm, 2.7 nm and 4.0 nm as the weight ratio of monomers/FDU-12 increases from 0.09 to 0.17 and to 0.35. Though the reduction in BET surface area, pore volume and pore diameter was observed, the composite samples still have much higher BET surface area (479 to 360 m^2/g) than TsDPEN-polymer prepared by polymerization of DVB and VBS-DPEN under similar conditions to polymer@silica composite materials but without FDU-12. This suggests that polymer could be dispersed in FDU-12 to increase

Table 1. Textural parameters, weight loss and S content of FDU-12 and polymer@silica composite materials.

Sample	Surface area (m^2/g) [a]	Pore volume (cm^3/g) [b]	Pore diameter (nm) [c]	Weight loss (wt%)[d]	S content (mmol/g) [e]
FDU-12	574	0.64	17.6	--	--
polymer@silica-0.09	479	0.48	14.6	8.9	0.227
polymer@silica-0.17	441	0.41	12.2	16.2	0.273
polymer@silica-0.35	392	0.35	9.5	26.6	0.360
polymer@silica-0.70	360	0.29	--	38.0	0.549
$Polymer_H$@silica-0.17	521	0.46	10.3	15.1	0.145
C_3-polymer@silica-0.17	387	0.36	10.7	21.8	0.205
N^+Cl^--polymer@silica-0.17	30	0.06	--	24.8	0.245
TsDPEN-polymer [f]	105	--	--	100	1.205

[a] BET surface area. [b] Single point pore volume calculated at relative pressure P/Po of 0.99. [c] BJH method from adsorption branch. [d] Weight loss between 250-800 °C from TG curves. [e] Calculated based on element analysis. [f] Prepared by polymerization of DVB and VBS-DPEN under similar conditions to polymer@silica composite materials but without FDU-12.

the BET surface area. After surface modification, further reduction in BET surface area, pore volume and pore diameter could be observed (Table 1). N^+Cl^--polymer@silica-0.17 affords very low BET surface area and pore volume of 30 m^2/g and 0.06 cm^3/g, respectively.

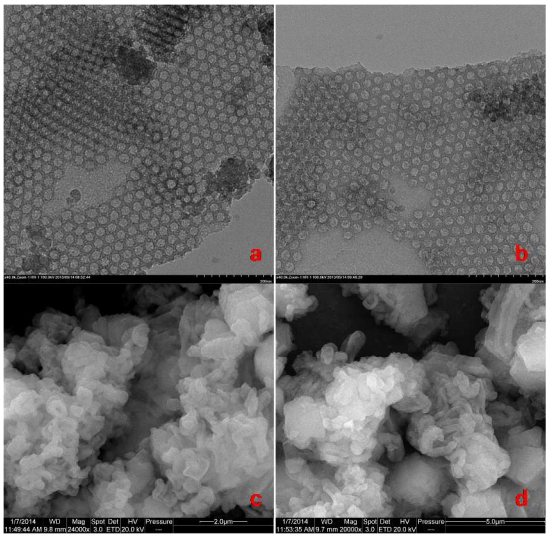

Figure 2. TEM (a, b) and SEM (c, d) images of (a, c) FDU-12 and (b, d) polymer@silica-0.17.

Transmission electron microscopy (TEM) investigation reveals that both FDU-12 and polymer@silica-0.17 have a uniform and well defined cubic mesostructure (Fm3m) (Figure 2). Bulk polymer formation was not found on the external surface of FDU-12, demonstrating that most of the monomers were polymerized inside the silica nanopores. The SEM images of FDU-12 and polymer@silica-0.17 show that they are both composed of irregularly shaped particles with size in the range of 1-4 um. No bulk polymers were found in the SEM image of polymer@silica-0.17, further demonstrating that most of the monomers were inside nanocages of FDU-12.

Composition characterization and thermal stability

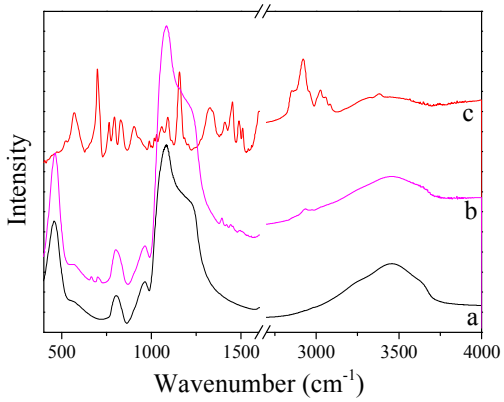

Figure 3. FT-IR spectra of (a) FDU-12, (b) polymer@silica-0.17, and (c) TsDPEN-polymer.

FT-IR spectra of representative samples, FDU-12, TsDPEN-polymer and polymer@silica-0.17, are displayed in Figure 3. Polymer@silica-0.17 exhibits the characteristic bands from silica at around 3456, 1650, and 1085 cm^{-1} respectively for ν (O-H), δ (O-H), and ω (Si-O). The weak bands at around 2800-2950 cm^{-1} are assigned to the C-H stretching vibrations and the bands at around 1450-1540 cm^{-1} and 650-730 cm^{-1} were attributed to the C=C vibration and breathing vibration of phenyl ring. All these observations demonstrate the successful incorporation of polymers in the mesosilica material.

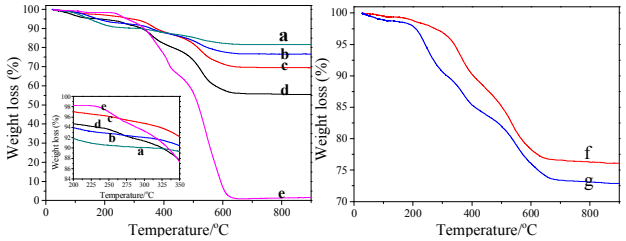

Figure 4. Thermogravimetric analysis of a) polymer@silica-0.09, b) polymer@silica-0.17, c) polymer@silica-0.35, d) polymer@silica-0.70, e) TsDPEN-polymer, f) C_3- polymer@silica-0.17, g) N^+Cl^--polymer@silica-0.17.

The thermal stability of polymer@silica was investigated using thermo gravimetric analysis (TGA) technique (Figure 4). The weight loss below 200 °C corresponds to the loss of physically adsorbed water. The weight loss between 250-800 °C is from the decomposition of polymer within nanopores. Via adjusting the monomer contents, the amount of polymer in polymer@silica could be varied in the range of 8.9% to 38% (Table 1). Interestingly, polymer@silica-0.17 and polymer@silica-0.09 with decomposition temperature higher than TsDPEN-polymer afford two consecutive steps of weight loss at 350 and 500 °C, while polymer@silica-0.70 and polymer@silica-0.35 shows three consecutive steps of weight loss at 250, 350 and 500 °C. The higher thermal stability of polymer@silica than TsDPEN-polymer is might from the strong interaction of polymer with silica. This also suggests that polymers are distributed uniformly in the pore for polymer@silica-0.17 and polymer@silica-0.09. The extra weight loss step at 250 °C for polymer@silica-0.35 and polymer@silica-0.70 is from the polymers with weak interaction with silica. The TG analysis shows that 16.2 wt% is the upper limit for the uniform distribution of polymers on the pore surface of FDU-12. After that, extra polymers may aggregate together. After surface modification with C_3 or N^+Cl^-, the slight increase in weight loss could be observed. This proved the successful incorporation of organic groups in polymer@silica using grafting method.

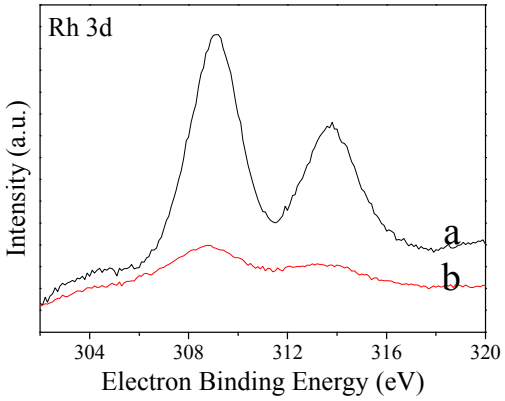

Figure 5. XPS spectra of (a) Cp*RhTsDPEN and (b) Rh-polymer@silica-0.17.

In order to demonstrate the coordination of metal precursor and investigate the electronic state of rhodium, X-ray photoelectron spectroscopy (XPS) are employed to characterize representative polymer@silica-0.17 after coordination with Rh precursor and homogeneous catalyst, Cp*RhTsDPEN. As shown in Figure 5, the solid catalyst has nearly the same $3d_{5/2}$ electron binding energy as parent Cp*RhTsDPEN (308.94 eV vs 309.04 eV), suggesting that Cp*RhTsDPEN within solid catalyst retained its original chiral coordination microenvironment.

Surface properties

The surface properties of Rh-polymer@silica were investigated using water contact angle and gas adsorption measurement which respectively provide the information of outer surface and inner pore surface of porous materials (Table 2). Rh-TsDPEN-polymer with water contact angle of 111° and adsorbed benzene/H_2O molar ratio of 1.53 has hydrophobic properties for both outer and inner surface. Rh-polymer@silica samples have lower water contact angle and adsorbed benzene/H_2O molar ratio than Rh-TsDPEN-polymer, showing the composite samples have more surface hydrophilicity due to the co-existence of hydrophilic silica and hydrophobic polymer. Irrespective of different polymer content, Rh-polymer@silica-x samples with $x \leq 0.35$ afford the same contact angle of 48°, showing that polymers are inside the pore and outer surface hydrophilicity/hydrophobicity is mainly determined by the silica. Rh-polymer@silica-0.70 with the largest water contact angle of 72° has some polymers on the outer surface. Rh-polymer@silica-x samples with $x \leq 0.35$ also have similar inner surface hydrophilic/hydrophobic properties as evidenced by the similar adsorbed benzene/H_2O molar ratio. Rh-polymer@silica-0.70 has more inner surface hydrophobicity than Rh-polymer@silica-x samples with $x \leq 0.35$. Rh-$polymer_H$@silica-0.17 gives similar water contact angle and adsorbed benzene/H_2O ratio to Rh-polymer@silica-0.17, indicating that the ratio of DVB and VBS-DPEN monomers does not affect the inner and outer surface properties of the composite materials.

Taking polymer@silica-0.17 as a model, the surface hydrophilicity/hydrophobicity was further modified through post-grafting with organic silane reagent, n-propyltrimethoxysilane (C_3) or N-trimethoxysilylpropyl- N, N, N-tri-n-butylammonium chloride (N^+Cl^-). Compared with Rh-polymer@silica-0.17, both the inner and outer surface hydrophobicity of Rh-polymer@silica-0.17 are greatly enhanced via propyl modification as evidenced by the increased water contact angle and adsorbed benzene/H_2O ratio. Notably, Rh-N^+Cl^--polymer@silica-0.17 shows lower water contact angle but higher adsorbed benzene/H_2O ratio than Rh-polymer@silica-0.17, suggesting that Rh-N^+Cl^--polymer@silica-0.17 could be well dispersed in water and also could adsorb hydrophobic substrates. This unique property is mainly attributed to the amphiphilic properties of N^+Cl^- moiety.

The catalytic performance of Rh-polymer@silica catalyst

The catalytic performance of polymer@silica composites was tested in the aqueous asymmetric transfer hydrogenation (ATH) of acetophenone and the catalytic results are presented in Table 2. The homogeneous Rh-TsDPEN could smoothly catalyze the reaction with 99% conversion and 95% ee. Rh-TsDPEN-polymer only gives 34 % conversion and 93% ee under identical reaction conditions. The poor activity might be related to its low BET surface area and hydrophobic surface properties which are not beneficial for the exposure of active site and for mass transport in aqueous solution. After adding $Bu_4N^+Br^-$ as phase transfer reagent, the mass transport could be improved, and the TOF is enhanced significantly from 13 to 130 h^{-1}. Notably, all Rh-polymer@silica catalysts in the absence of $Bu_4N^+Br^-$ show much higher activity than Rh-TsDPEN-polymer in the presence of $Bu_4N^+Br^-$. The ee value is almost the same for both homogeneous and Rh-polymer@silica catalysts. Rh-polymer@silica samples with outer surface hydrophilicity could be well dispersed in water and the existence of polymers in the pore could favor the enrichment of hydrophobic substrate. Thus, Rh-polymer@silica samples could efficiently catalyze the ATH reaction even without the addition of phase transfer reagents. Also, the high catalytic performance of Rh-polymer@silica samples is related with their high BET surface area which could increase the exposure degree of the active sites.

Rh-polymer@silica-0.17 affords the highest TOF of 468 h^{-1} and Rh-polymer@silica-0.70 shows the lowest TOF of 148 h^{-1} among Rh-polymer@silica samples. With polymer/FUD-12 ratio increases from 0.09 to 0.35, the TOF of Rh-polymer@silica samples increases from 250 to 468 h^{-1} and then decreases to 156 h^{-1}. The three samples have similar inner and outer surface properties, thus the different activity is mainly related with the surface area and exposure degree of active sites. Rh-polymer@silica-0.09 and Rh-polymer@silica-0.17 have comparable BET surface area and pore volume. The increase in the polymer content benefits the higher activity, probably due to high concentration of active sites. However, furthering increasing

Table 2. The surface properties of Rh-polymer@silica and their catalytic performance in the asymmetric transfer hydrogenation of acetophenone. [a]

Catalyst	Water contact angle (°)	Adsorbed benzene/H_2O (mol ratio)	Rh (mmol/g)	Conv (%)[b]	Ee (%)[b]	TOF (h^{-1})[c]
Rh-TsDPEN	--	--	--	>99	95	340
Rh-TsDPEN-polymer[d]	111	1.53	0.572	34 (73)	93 (95)	13 (130)
Rh-polymer@silica-0.09	48	0.28	0.049	92	95	250
Rh-polymer@silica-0.17	48	0.24	0.074	>99	94	468
Rh-plymer@silica-0.35	48	0.29	0.136	72	93	156
Rh-polymer@silica-0.70	72	0.36	0.180	64	94	148
Rh-$polymer_H$@silica-0.17	49	0.26	0.034	>99	94	585
Rh-C_3-polymer@silica-0.17	76	0.71	0.100	67	95	48
Rh-N^+Cl^--polymer@silica-0.17	30	0.74	0.012	>99	95	561

[a] Reaction conditions: solid catalyst (2.5 μmol Rh), HCOONa (0.17 g, 2.5 mmol), acetophenone (0.5 mmol) and 2.0 ml H_2O, reaction temperature (313 K), 1000 r/min, for 3 h. [b] Analysis by GC, the reaction time for the final conversion is 3 h. [c] Turnover frequency is calculated with conversion of acetophenone less than 20%. [d] Data in parenthesis are obtained in the presence of $Bu_4N^+Br^-$.

the polymer content, the decrease in the TOF could be observed. This is probably due to low BET surface area and the aggregation of some polymers which decreases the exposure degree of active sites. Moreover, the increased outer surface hydrophobicity may also cause the decrease of the activity.

Interestingly, after varying the molar ratio of the monomers (DVB/VBS-DPEN), the obtained catalyst Rh-polymer$_H$@silica-0.17 exhibited higher activity than Rh-polymer@silica-0.17. Considering the fact that the two samples have similar inner and outer surface properties, its higher activity might be related with the larger BET surface area and pore volume resulted by the decreasing of the content of monomer VBS-DPEN with large size. For another, the resulted decreasing of Rh density and the increasing of hydrophobic DVB monomers might also be beneficial for the exposure of active sites and the enrichment of hydrophobic substrate. All these factors result the high catalytic performance of Rh-polymer$_H$@silica-0.17. And under identical reaction conditions, Rh-polymer$_H$@silica-0.17 is 45 fold as active as Rh-TsDPEN-polymer and is 1.7 fold as active as the homogeneous counterpart. After reaction, the metal leaching was measured via ICP, and about 0.3 ppm Rh was found in the reaction solution. This result also reveals that the reaction was mainly catalyzed by the solid catalyst.

Rh-C_3-polymer@silica-0.17 affords much lower TOF than Rh-polymer@silica-0.17 (TOF: 48 versus 468 h^{-1}), showing propyl modification does not favor to increase the activity. This is due to the combined effect of the decrease in surface area and pore volume and the increase in outer surface hydrophobicity. On the contrary, Rh-N^+Cl^--polymer@silica-0.17 is much more active than Rh-polymer@silica-0.17 (TOF: 561 versus 468 h^{-1}) though the former sample has very low BET surface area and pore volume. This result is similar with our previous report.[14] However, compared with encapsulation method we reported previously, no extra modification of pore entrance size is needed in this work to prevent the leaching of active sites because TsDPEN was cross-linked in the polymer. Moreover, the solid catalyst could afford high TOF even without the presence of N^+Br^- due to the fact that the solid catalyst has unique outer surface hydrophilicty and inner surface hydrophobicity.

Table 3. Asymmetric transfer hydrogenation of substituted aromatic ketone using Rh-polymer$_H$@silica-0.17 as solid catalyst. [a]

Entry	Ar	Reaction time (h)	Conv.(%)[b]	Ee. (%)[b]
1	Ph	3	>99	94
2	4-FPh	3	>99	93
3	3-Br	3	>99	92
4	4-ClPh	3	>99	93
5	3-OMe	3	99	92
6	4-Me	4	94	88

[a] Reaction conditions: solid catalyst (2.5 μmol Rh), HCOONa (0.17 g, 2.5 mmol), ketone (0.5 mmol) and 2.0 ml H_2O, reaction temperature (313 K), 1000 r/min. [b] Analysis by GC.

Encouraged by the superior performance of Rh-polymer@silica, other ketones have been intensively used in ATH reactions with Rh-polymer$_H$@silica-0.17 as model catalyst (Table 3). All ketones tested could be efficiently converted into chiral alcohols with high ee values on Rh-polymer$_H$@silica-0.17. Electron-rich aromatic ketones can also be reduced to corresponding alcohols with high activity and ee value, although a longer time is needed compared with electron-deficient aromatic ketones.

The stability of the chiral solid catalyst was investigated using Rh-polymer$_H$@silica-0.17 as a model catalyst in the ATH of acetophenone (Figure 6). The solid catalyst can be easily recovered via simple centrifugation and can be reused more than 6 times with little loss of enantioselectivity though longer reaction time is needed to obtain high conversion during the recycle process. The gradual decrease in activity is probably due to the deterioration of chiral catalysts during the recycle process.

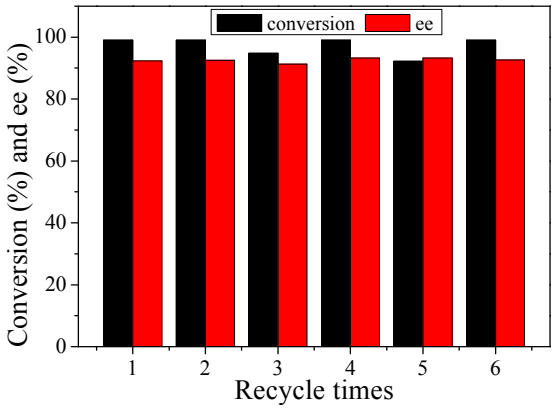

Figure 6. Recyclability of Rh-polymer$_H$@silica-0.17 in the asymmetric transfer hydrogenation of acetophenone (the reaction time for cycle 1, 2, 3, 4, 5, and 6 is 3 h, 3 h, 5 h, 8 h,10 h, 14 h, respectively).

Conclusions

In summary, we have reported a new strategy for the immobilization of Noyori-Ikariya catalyst by forming polymer@silica composite catalysts. With polymer content less than 16.2 wt%, the composites with polymers uniformly distributed in the nanopore of FDU-12 could be obtained. Under optimized conditions, the composite material could efficiently catalyze the aqueous ATH of ketone and afford much higher activity than homogeneous counterparts due to the fact that the composite with hydrophilic outer and hydrophobic inner surface properties could facilitate the mass transfer of hydrophobic substrate in water. Moreover, the solid catalyst could be facilely separated and recycled. This novel strategy could be extended to other water-oil-solid tri-phase reaction systems.

Acknowledgements

This work was financially supported by NSFC (21325313, 21232008, 21273226, 21321002) and by the key research program of the Chinese Academy of Sciences.

Notes and references

[a] *State Key Laboratory of Catalysis, Dalian Institute of Chemical Physics, Chinese Academy of Sciences, 457 Zhongshan Road, Dalian 116023, China*

[b] *University of Chinese Academy of Sciences, Beijing 100049, China*

** To whom correspondence should be addressed. E-mail: yangqh@dicp.ac.cn; Fax: 86-411-84694447. URL: http://www.hmm.dicp.ac.cn*

1. R. Noyori and S. Hashiguchi, *Accounts Chem Res*, 1997, 30, 97-102.
2. T. Ikariya and A. J. Blacker, *Accounts Chem Res*, 2007, 40, 1300-1308.

3. C. Wang, B. Villa-Marcos and J. L. Xiao, *Chem Commun*, 2011, 47, 9773-9785.
4. P. A. Dub and T. Ikariya, *J Am Chem Soc*, 2013, 135, 2604-2619.
5. X. F. Wu, X. G. Li, F. King and J. L. Xiao, *Angew Chem Int Edit*, 2005, 44, 3407-3411.
6. J. H. Li, Y. F. Tang, Q. W. Wang, X. F. Li, L. F. Cun, X. M. Zhang, J. Zhu, L. C. Li and J. G. Deng, *J Am Chem Soc*, 2012, 134, 18522-18525.
7. J. Li, Y. M. Zhang, D. F. Han, Q. Gao and C. Li, *J Mol Catal a-Chem*, 2009, 298, 31-35.
8. G. H. Liu, H. Y. Gu, Y. Q. Sun, J. Long, Y. L. Xu and H. X. Li, *Adv Synth Catal*, 2011, 353, 1317-1324.
9. X. G. Li, X. F. Wu, W. P. Chen, F. E. Hancock, F. King and J. L. Xiao, *Org Lett*, 2004, 6, 3321-3324.
10. N. Haraguchi, A. Nishiyama and S. Itsuno, *J Polym Sci Pol Chem*, 2010, 48, 3340-3349.
11. Y. Arakawa, N. Haraguchi and S. Itsuno, *Tetrahedron Lett*, 2006, 47, 3239-3243.
12. P. N. Liu, J. G. Deng, Y. Q. Tu and S. H. Wang, *Chem Commun*, 2004, 2070-2071.
13. N. Haraguchi, K. Tsuru, Y. Arakawa and S. Itsuno, *Org Biomol Chem*, 2009, 7, 69-75.
14. S. Y. Bai, H. Q. Yang, P. Wang, J. S. Gao, B. Li, Q. H. Yang and C. Li, *Chem Commun*, 2010, 46, 8145-8147.
15. B. Deng, W. Xiao, C. Li, F. Zhou, X. Xia, T. Cheng and G. Liu, *J Catal*, 2014, 320, 70-76.
16. D. Xia, T. Cheng, W. Xiao, K. Liu, Z. Wang, G. Liu, H. Li and W. Wang, *Chemcatchem*, 2013, 5, 1784-1789.
17. J. Wei, X. M. Zhang, X. M. Zhang, Y. P. Zhao, R. X. Li and Q. H. Yang, *Chemcatchem*, 2014, 6, 1368-1374.
18. Y. L. Xu, T. Y. Cheng, J. Long, K. T. Liu, Q. Q. Qian, F. Gao, G. H. Liu and H. X. Li, *Adv Synth Catal*, 2012, 354, 3250-3258.
19. R. Liu, T. Y. Cheng, L. Y. Kong, C. Chen, G. H. Liu and H. X. Li, *J Catal*, 2013, 307, 55-61.
20. H. S. Zhang, R. H. Jin, H. Yao, S. Tang, J. L. Zhuang, G. H. Liu and H. X. Li, *Chem Commun*, 2012, 48, 7874-7876.
21. F. Gao, R. H. Jin, D. C. Zhang, Q. X. Liang, Q. Q. Ye and G. H. Liu, *Green Chem*, 2013, 15, 2208-2214.
22. Q. Sun, Y. Y. Jin, L. F. Zhu, L. Wang, X. J. Meng and F. S. Xiao, *Nano Today*, 2013, 8, 342-350.
23. M. Choi, F. Kleitz, D. N. Liu, H. Y. Lee, W. S. Ahn and R. Ryoo, *J Am Chem Soc*, 2005, 127, 1924-1932.
24. G. J. A. A. Soler-Illia and O. Azzaroni, *Chem Soc Rev*, 2011, 40, 1107-1150.
25. S. Banerjee, T. K. Paira, A. Kotal and T. K. Mandal, *Adv Funct Mater*, 2012, 22, 4751-4762.
26. R. Alamillo, A. J. Crisci, J. M. R. Gallo, S. L. Scott and J. A. Dumesic, *Angew Chem Int Edit*, 2013, 52, 10349-10351.
27. M. Windbergs, Y. Zhao, J. Heyman and D. A. Weitz, *J Am Chem Soc*, 2013, 135, 7933-7937.
28. A. Abbaspourrad, N. J. Carroll, S. H. Kim and D. A. Weitz, *Adv Mater*, 2013, 25, 3215-3221.
29. R. Guillet-Nicolas, L. Marcoux and F. Kleitz, *New J Chem*, 2010, 34, 355-366.
30. J. Fan, C. Z. Yu, T. Gao, J. Lei, B. Z. Tian, L. M. Wang, Q. Luo, B. Tu, W. Z. Zhou and D. Y. Zhao, *Angew Chem Int Edit*, 2003, 42, 3146-3150.

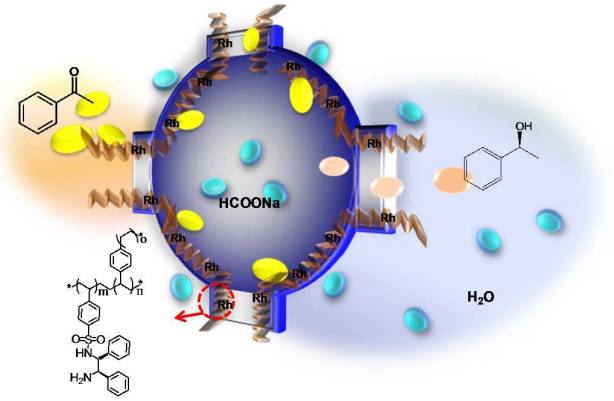

The polymer@silica composites with tunable outer and inner surface properties could efficiently catalyze the asymmetric transfer hydrogenation (ATH) of ketones in aqueous medium.